UNIVERSITA' DI NAPOLI FEDERICO II

DOTTORATO DI RICERCA
BIOCHIMICA E BIOLOGIA CELLULARE E MOLECOLARE
XXIV CICLO

The glutathione biosynthesis in the psychrophile *Pseudoalteromonas haloplanktis*

Antonella Albino

Relatore
Prof. Emmanuele De Vendittis

Coordinatore
Prof. Paolo Arcari

Correlatore
Prof. Mariorosario Masullo

ANNO ACCADEMICO 2010/2011

Ringraziamenti e dediche

Ce l'ho fatta...ho raggiunto questo traguardo tanto desiderato!!!
E ora è con piacere che dedico questa breve ma intensa pagina alle persone care che mi hanno accompagnata durante questi 3 anni di dottorato.

Ricordo ancora quando nel Gennaio del 2009 giunsi al 6° piano della Torre Biologica.

Nessuno mi conosceva, ero un'estranea, eppure sin dall'inizio tutti i docenti mi hanno accolta come una figlia.
Primo fra tutti ringrazio con grande affetto e gratitudine la mia guida, il prof. E. De Vendittis, una persona buona e paziente, il mio maestro non solo di studi, ma anche di vita che con i suoi saggi consigli mi ha tanto aiutato e sostenuto. Ringrazio di cuore, inoltre, il buon prof. M. Masullo per i suoi consigli tecnici e per la sua completa disponibilità, insieme al prof. Arcari, ai ricercatori R. Rullo, R. Ruocco, L. Rippa, G. Corso e A. Lamberti e ai colleghi (Salvatore, Alessandra e Alberto) che costituiscono il gruppo di ricerca con cui ho lavorato. I miei ringraziamenti vanno anche agli altri colleghi (tesisti, dottorandi e specializzandi) del 6° piano della Torre Biologica.
Ringrazio la simpaticissima Alba che si è messa sempre a disposizione per qualsiasi problema.

Quanti sacrifici ho fatto, ho affrontato difficoltà e incomprensioni: un cammino che, però, per me rappresenta la speranza di un futuro professionale che ho sempre sognato. Ho condiviso risate e tensioni,

momenti positivi e negativi con tutti, anche se non ho potuto trascorrere molto tempo in loro compagnia. Ringrazio tutti!!!
Ringrazio, infine, i miei genitori, le mie sorelle (Stefania, Tania e Imma), mia nonna Concetta e Angelo che mi hanno sempre incoraggiato ad andare avanti e ad inseguire la mia passione!!

RIASSUNTO

Il glutatione ridotto (GSH), insieme alla sua forma ossidata (GSSG), costituisce il più efficace sistema antiossidante preposto al controllo dello stato redox cellulare. La sua biosintesi a partire da glutammato, cisteina e glicina, richiede di norma l'intervento di due enzimi: il primo, la γ-glutamil-cisteina ligasi (GshA), forma la γ-glutamil-cisteina, mentre il secondo, la glutatione sintetasi (GshB), porta alla formazione di GSH. Nel genoma di *Pseudoalteromonas haloplanktis,* un eubatterio psicrofilo isolato dal mare antartico, sono stati putativamente identificati due geni codificanti per GshA (*Ph*GshA-I e *Ph*GshA-II) ed un unico gene per la GshB (*Ph*GshB). Lo studio delle proprietà biochimiche di tali enzimi è stato affrontato con un adatto sistema di espressione eterologa, che ha permesso di ottenere le forme ricombinanti di *Ph*GshB e *Ph*GshA-II (r*Ph*GshB e r*Ph*GshAII), purificate mediante cromatografia per affinità grazie alla fusione con una coda di istidine.

Il primo enzima oggetto di studio è stato r*Ph*GshB. La sua purificazione è stata realizzata sia in assenza che in presenza di β-mercaptoetanolo. Dallo studio delle sue proprietà molecolari è emerso che quando r*Ph*GshB è purificato in presenza di β-mercaptoetanolo, subisce una modifica covalente da parte dell'agente riducente, che però non influenza significativamente le sue proprietà biochimiche. È stata poi determinata la massa molecolare di r*Ph*GshB sia in condizioni denaturanti che native. In condizioni denaturanti il valore

di 36 kDa corrisponde alla massa del monomero di *Ph*GshB, mentre in condizioni native la massa determinata mediante gel-filtrazione oscilla tra 74 e 136 kDa, valori corrispondenti rispettivamente ad un'organizzazione omodimerica o omotetramerica. Il diverso comportamento cromatografico dipende dalla concentrazione dell'enzima ed i dati ottenuti suggeriscono che a più alte concentrazioni si forma un tetrametro poco stabile, che a più basse concentrazioni si converte in una struttura dimerica più stabile.

Per studiare l'attività di r*Ph*GshB, è stato messo a punto un nuovo metodo di dosaggio diretto, basato sull'idrolisi del substrato radioattivo [γ^{32}P]ATP, poiché la sintesi del GSH catalizzata da GshB è accoppiata alla reazione di idrolisi dell'ATP in ADP e fosfato inorganico. L'attività ATPasica di r*Ph*GshB richiede la presenza degli altri due substrati, glicina e γ-glutammilcisteina (γ-Glu-Cys). r*Ph*GshB manifesta la sua massima attività ad un pH compreso tra 7,4 e 8,2; inoltre è necessaria la presenza di un catione divalente e con 5 mM Mg^{++} si raggiunge la massima attività.

Sono stati poi determinati i parametri cinetici di r*Ph*GshB alla temperatura di 15°C, valore ottimale per la crescita di *P. haloplanktis*. L'enzima possiede un'affinità comparabile per i substrati ATP e γ-Glu-Cys (K_m= 0,26 e 0,25 mM, rispettivamente), mentre per la glicina possiede un'affinità inferiore (K_m= 0,75 mM). Il confronto di questi dati con quelli del corrispondente enzima da altre sorgenti evidenzia la notevole similarità con *Escherichia coli* e un'analoga minore affinità

per la glicina rispetto agli altri due substrati nelle altre fonti. Studi di inibizione enzimatica hanno poi evidenziato che GSSG agisce da inibitore di r*Ph*GshB. È stato poi valutato l'effetto della temperatura sui parametri cinetici di r*Ph*GshB relativi al substrato ATP nell'intervallo di temperatura 10-30 °C. Dai dati ottenuti è emerso che r*Ph*GshB è già attivo a 10°C e che la sua V_{max} cresce significativamente all'aumentare della temperatura almeno fino a 25°C; d'altra parte, nell'intervallo di temperatura considerato, la K_m oscilla solo tra 0,17 e 0,28 mM. Ciò ha reso possibile l'analisi dei valori di k_{cat} secondo il plot di Arrhenius. Nell'intervallo di linearità del plot (10-25°C) è stata calcolata un'energia di attivazione di 75 kJ/mol, un valore abbastanza elevato per un enzima psicrofilo.

La termostabilità di r*Ph*GshB è stata analizzata mediante un profilo di inattivazione termica da cui è stata estrapolata una semivita di 10 min a 50,5°C, un valore leggermente elevato per un enzima psicrofilo, anche se non insolito per enzimi preposti al controllo dello stato redox cellulare. Sono stati poi determinati i parametri energetici del processo di inattivazione termica. Il valore di 208 kJ/mol calcolato per l'energia di attivazione di tale processo è intermedio tra quelli normalmente ottenuti per enzimi psicrofili e mesofili.

Infine, grazie alla messa a punto di una particolare tecnica di cristallizzazione, è stato possibile ottenere forme cristalline di r*Ph*GshB, risultate idonee per lo studio della struttura tridimensionale dell'enzima mediante diffrazione ai raggi X.

Si è passati poi alla caratterizzazione biochimica di r*Ph*GshA-II, l'altro enzima preposto alla biosintesi del glutatione, impiegando lo stesso tipo di dosaggio già utilizzato per r*Ph*GshB, poiché anche l'attività di GshA è accoppiata ad una ATPasi. I dati preliminari ottenuti dimostrano che l'attività enzimatica di r*Ph*GshA-II richiede necessariamente un ambiente riducente e la presenza degli altri due substrati glutammato e cisteina. Infine per l'attività di r*Ph*GshA-II è indispensabile la presenza di concentrazioni più elevate del catione Mg^{++} (10-20 mM) rispetto a quelle già determinate per r*Ph*GshB. Quando sarà completata la caratterizzazione molecolare e biochimica di *Ph*GshA-II, sarà possibile ricostituire in vitro per la prima volta il sistema per la biosintesi del glutatione in un organismo psicrofilo.

SUMMARY

Reduced glutathione (GSH), together with its oxidized form (GSSG), is the most effective antioxidant system responsible for controlling the cellular redox state. Its biosynthesis from glutamate, cysteine and glycine, normally requires two enzymes. Indeed, γ-glutamyl-cysteine ligase (GshA) forms γ-glutamyl-cysteine, whereas glutathione synthetase (GshB) leads to the formation of GSH. In the genome of *Pseudoalteromonas haloplanktis*, a psychrophilic eubacterium isolated from Antarctic sea water, two genes coding for GshA (*Ph*GshA-I and *Ph*GshA-II) and one gene for GshB (*Ph*GshB) were putatively identified. The study of the biochemical properties of these enzymes was addressed with an appropriate heterologous expression system, thus leading to the production of the recombinant forms of *Ph*GshB and *Ph*GshA-II (r*Ph*GshB and r*Ph*GshA-II), purified by affinity chromatography.

The first enzyme investigated was r*Ph*GshB. Its purification was achieved either in the absence or in the presence of β-mercaptoethanol. The study of its molecular properties showed that, when purified in the presence of β-mercaptoethanol, r*Ph*GshB underwent a covalent modification; however, this modification did not significantly affect its biochemical properties. The molecular mass of r*Ph*GshB in denaturing conditions was 36 kDa, corresponding to the mass of the *Ph*GshB monomer; in non denaturing conditions the mass determined by gel-filtration ranged between 74 and 136 kDa,

respectively, values corresponding to a dimeric or tetrameric organization. The different behavior depended on the enzyme concentration and the data suggested that at higher concentrations the enzyme formed an unstable tetramer that at lower concentrations was converted into a dimeric and more stable form.

To study the activity of r*Ph*GshB, a new method for direct determination was developed, based on the hydrolysis of the radioactive substrate [γ^{32}P] ATP; in fact, the synthesis of GSH catalyzed by GshB is coupled to the hydrolysis of ATP. The ATPase activity of r*Ph*GshB required the presence of the other two substrates, glycine and γ-glutamylcysteine (γ-Glu-Cys). r*Ph*GshB showed its maximum activity in the 7.4-8.2 pH range. The enzyme activity required also the presence of a divalent cation and at 5 mM Mg^{++} reached its maximum.

The kinetic parameters of r*Ph*GshB at 15°C, the optimum value for growth of *P. haloplanktis*, were determined. The enzyme showed a comparable affinity for ATP and γ-Glu-Cys (K_m = 0.26 mM and 0.25 mM, respectively), whereas a lower affinity was determined for glycine (K_m = 0.75 mM). The comparison of these data with those of the corresponding enzyme from other sources showed the remarkable similarity with *Escherichia coli*; a similar lower affinity for glycine compared to the other two substrates was found in the other sources. Enzyme inhibition studies showed that GSSG is an inhibitor of r*Ph*GshB. The effect of temperature on the kinetic parameters of

r*Ph*GshB was analysed in the temperature range 10-30°C. The data showed that r*Ph*GshB is already active at 10°C and its V_{max} significantly increased with temperature up to 25°C; on the other hand, in the temperature interval considered, a minimum variation of K_m was observed. The k_{cat} values were then used to draw an Arrhenius plot and in the range of linearity (10-25°C) an activation energy of 75 kJ/mol was determined, a value quite high for a psychrophilic enzyme.

The thermostability of r*Ph*GshB was analyzed using a thermal inactivation profile and an extrapolated half-life of 10 min at 50.5°C was derived. This value was slightly high for a psychrophilic enzyme, although not unusual for enzymes involved in the control of the cellular redox state. A value of 208 kJ/mol was calculated for the energy of activation of the heat inactivation process; this value was intermediate between those usually obtained for psychrophilic and mesophilic enzymes, respectively.

Finally, the development of a new crystallization technique allowed the obtainment of crystal forms of r*Ph*GshB, useful for the determination of the three-dimensional structure of the enzyme by X-ray diffraction.

The biochemical characterization of r*Ph*GshA-II was started, using the same assay adopted for r*Ph*GshB. Preliminary data obtained showed that the enzyme activity of r*Ph*GshA-II requires a reducing agent in the reaction mixture; furthermore, the presence of the other

two substrates glutamate and cysteine, is also required. The activity of r*Ph*GshA-II needed a higher concentration of Mg^{++} (10-20 mM) compared to that already determined for r*Ph*GshB. When the characterization of the molecular and biochemical properties of *Ph*GshA-II will be completed, it will be possible to reconstitute *in vitro* for the first time the system for the biosynthesis of glutathione in a psychrophilic organism.

INDEX

Index of Figures

Index of Tables

INTRODUCTION

Glutathione (GSH) is an abundant low molecular weight thiol, which displays its antioxidant cellular functions in virtually all eukaryotes[1–5] and also in many prokaryotes.[6–10] Several investigations demonstrated that GSH is the main regulator of the physiological redox environment through an intracellular balance with its oxidised form (GSSG).[5,10] Defence against oxidative damages, detoxification of foreign compounds, and protection of protein sulfhydryls from irreversible oxidation are among the most common antioxidant functions exerted by the GSH/GSSG redox couple. On the other hand, GSH, GSSG and/or S-nitrosoglutathione (GSNO) are responsible for the S-thiolation reaction, a covalent modification forming a glutathionyl adduct on reactive cysteine residues and possibly regulating the function of the target protein.[11–13]

In both eukaryotes and prokaryotes the biosynthesis of this tripeptide takes place through an enzyme system including two sequential reactions, each of them driven by a coupled ATPase activity.[1] In the first reaction, the enzyme glutamyl–cysteine ligase (GshA) catalyses the formation of L–γ–glutamylcysteine (γ–Glu–Cys) from L–glutamate and L–cysteine; in the second one, another enzyme, glutathione synthetase (GshB) leads to the formation of GSH from γ–Glu–Cys and glycine, as reported in the following scheme.

$$\text{L–glutamate + L–cysteine + ATP} \xrightarrow{\text{GshA}} \text{γ–Glu–Cys + ADP + } P_i \qquad (1)$$

$$\text{γ–Glu–Cys + glycine + ATP} \xrightarrow{\text{GshB}} \text{GSH + ADP + } P_i \qquad (2)$$

Some organisms contain a single bifunctional enzyme possessing both activities displayed by GshA and GshB.[14–16] The rate limiting step of the whole process is reaction (1),[17] which is also feedback inhibited by GSH.[18,19] In both catalysed reactions, one ATP molecule is hydrolysed to ADP and inorganic phosphate in the presence of Mg^{2+} or Mn^{2+}, although with a different specificity towards the respective substrates.[20,21]

Biosynthesis of GSH and its functional role have been the object of several investigations in eukaryotes. In prokaryotes GSH is biosynthesized in almost all Gram-negative bacteria,[6] although its antioxidant role is somehow controversial. Indeed, GSH acts as a sacrificial nucleophile for the detoxification of chlorine compounds;[22] vice versa, it is dispensable for resistance to H_2O_2 and γ-radiation.[23] A diversified picture emerges for Gram-positive bacteria; indeed, GSH is absent is some anaerobic or microaerophilic sources,[6] it is replaced by other thiols in actinomycetes,[9] or it is produced through a bifunctional enzyme in *Streptococcus agalactiae*,[14] *Listeria monocytogenes*,[15] or *Pasteurella multocida*;[16] furthermore, in *Streptococcus mutans*, GSH is taken up from the external medium,

although the microorganism possesses the gene encoding a bifunctional enzyme.[24]

To our knowledge, glutathione biosynthesis was never reported in a cold-adapted source, where the antioxidant role of GSH could be more relevant for the survival of the psychrophilic source at cold temperatures. *Pseudoalteromonas haloplanktis* TAC125 is a psychrophilic eubacterium isolated form the Antarctic sea, growing in the 4-20°C temperature interval.[25] The presence of GSH in this Gram-negative gamma-proteobacterium was inferred by previous works, in which glutathionyl adducts were formed on enzymes involved in the redox balance of *P. haloplanktis*, such as superoxide dismutase[26] and thioredoxin reductase.[27] Furthermore, in case of superoxide dismutase, the covalent modification regulated the function of the antioxidant enzyme.[26]

The object of the present thesis is the enzyme system aimed at GSH biosynthesis in *P. haloplanktis*. In particular, the research was first focused on the production and characterization of a recombinant form of glutathione synthetase (r*Ph*GshB). A direct assay, based on the hydrolysis of radiolabelled ATP coupled to GSH formation, was set up for measuring the r*Ph*GshB activity. Using this assay, the kinetic parameters for each substrate were measured and the effect of temperature on enzyme activity and stability was evaluated. The research was then enlarged to the other enzyme involved in the GSH biosynthesis. Under this concern, owing to the occurrence of two

putative genes encoding GshA in the *P. haloplanktis* genome (*Ph*GshA-I and *Ph*GshA-II), it was decided to obtain a recombinant form of *Ph*GshA-II (r*Ph*GshA-II), sharing a higher percentage of amino acid identity with the single GshA from *Escherichia coli*. However, only preliminary data were obtained on the characterization of r*Ph*GshA-II.

The results obtained in this thesis represent the first investigation on the byosynthetic route of GSH in a psychrophilic source and prove that the functionality of a key reaction aimed at GSH biosynthesis is relevant even in cold-adapted microorganims.

MATERIALS AND METHODS

2.1 Materials

Restriction and modifying enzymes were from GE Healthcare or Promega. *Taq* DNA polymerase from Takara was used in PCR experiments. Plasmid pGEM–T Easy was from Promega, whereas vectors pET-28a(+), pET-22b(+) and the *Escherichia coli* BL21(DE3) strain were from Novagen. Purification of plasmids and DNA fragments was realised with Qiagen kits from M–Medical. Oligonucleotide synthesis, nucleotide sequencing and synthesis of vectors was carried out at Primm (Italy). Ampicillin, kanamycin, isopropyl-β-thiogalactopiranoside (IPTG), dithiothreitol (DTT), b–mercaptoethanol, γ–Glu–Cys and 5,5'–dithiobis–2–nitrobenzoic acid (DTNB) were from Sigma-Aldrich. [γ^{32}P]ATP (2 mCi mL^{-1}; 10 Ci $mmol^{-1}$) was purchased from Perkin Elmer. The chromatographic medium Ni–NTA agarose was from Qiagen. HPLC–grade solvents for mass spectrometry were obtained from Carlo Erba. All other chemicals were of analytical grade.

The following buffers were used: buffer A, 20 mM Tris•HCl, pH 7.8, 5 mM $MgCl_2$, 150 mM KCl, 20 mM imidazole•HCl; buffer B, 20 mM Tris•HCl, pH 7.8, 50% (v/v) glycerol; buffer C, 100 mM Tris•HCl, pH 7.8, supplemented with 5 mM $MgCl_2$ and 150 mM KCl; buffer D, 20 mM Tris•HCl, pH 7.8, 150 mM KCl.

2.2 Vectors for the expression of the genes coding *Ph*GshB and *Ph*GshA-II

The genomic DNA from *P. haloplanktis*, strain TAC125, contains a single putative gene encoding *Ph*GshB and two putative genes encoding *Ph*GshA genes, *Ph*GshA-I and *Ph*GshA-II, located on chromosome I and II, respectively. The gene encoding *Ph*GshB was amplified by PCR, using as template the genomic DNA of *P. haloplanktis* and the following synthetic oligonucleotides designed on the basis of the nucleotide sequences of the corresponding gene:

5'd-A_{-12}AGGCACAGCCC•*ATG*•GCA•ATT_{9}-3' (direct primer)

5'd-A_{960}AC•GCT•AAC•CTC•GAG•AGC•GAG•TCG•T_{936}-3'(reverse primer)

Numbering in primers begins from starting codon (italics), whereas underlined letters indicate mismatches introduced to create the *Nco*I and *Xho*I restriction sites. The obtained PCR product was cloned into the plasmid pGEM-T Easy and sequenced to confirm the identity of the *Ph*GshB gene. After digestion of recombinant plasmid with *Nco*I and *Xho*I, the resulting segment, containing the *Ph*GshB gene, was cloned into the prokaryotic expression vector pET-28a(+) digested with the same restriction enzymes. The new construct was controlled by restriction analysis and named v*Ph*GshB.

An identical strategy was followed for the heterologous expression of the gene encoding *Ph*GshA-II. The oligonucleotides used for PCR amplification were:

5'd-A_{-15}TTACAGAGGTTCATATG•ACG•TTA•T_{10}-3' (direct primer)

3'd-T_{1528}•GCT•CTT•TTG•CTC•GAG•CTT•ACC•TTC•T_{1503}-3' (reverse primer)

The amplified DNA segment was subcloned in the plasmid pGEM-T Easy and then cloned into the prokaryotic expression vector pET-22b(+) using the restriction enzymes *Nde* and *Xho*I. The new construct was named v*Ph*GshA-II.

2.3 Heterologous expression of the genes encoding *Ph*GshB and *Ph*GshA-II genes

The genomic DNA from *P. haloplanktis*, strain TAC125, was prepared as previously described.[28] Transformation of bacterial strains, preparation of plasmids and other details of DNA recombinant technology were carried out according to standard procedurs.[29] Expression of the vector v*Ph*GshB occurred in the host strain BL21(DE3) from *E. coli* under the control of IPTG induction. Moreover, in the recombinant *Ph*GshB (r*Ph*GshB), the C–terminal lysine of the endogenous enzyme was replaced by the extrapeptide $LE(H)_6$, useful for the one–step purification of the expression product by affinity chromatography. The following procedure modified and integrated a previously described protocol for the purification of r*Ph*GshB.[30] A colony obtained from the BL21(DE3)/v*Ph*GshB transformation was grown at 37°C in 1 L of LB medium containing 0.06 mg mL^{-1} kanamycin up to 0.6 OD_{600} and, upon the addition of 0.1 mg mL^{-1} IPTG, heterologous expression of the cloned gene was induced for 2 hours.

The culture was divided in two 500–mL aliquots and cells were collected by centrifugation at 5000 rpm for 20 min. One bacterial pellet was resuspended in 20 mL buffer A (non–reducing buffer), whereas the other one was resuspended in 20 mL buffer A supplemented with 7 mM β–mercaptoethanol (reducing buffer). After cellular lysis by French Press (Aminco, USA) and centrifugation at 30,000x*g*, two supernatants were obtained and each of them was added in batch to 3 mL of Ni–NTA Agarose resin, equilibrated with the non–reducing or reducing buffer, respectively. After incubation overnight at 4°C, each slurry was poured in a column, which was extensively washed with the corresponding buffer.

The bound r*Ph*GshB was then eluted by raising the imidazole•HCl concentration up to 200 mM to either non–reducing or reducing buffer. Pure protein fractions, as analysed by SDS–polyacrylamide gel elecrophoresis, were pooled together, eventually concentrated by ultrafiltration, and stored at –20°C in buffer B (non–reducing storage buffer) or buffer B supplemented with 7 mM β–mercaptoethanol (reducing storage buffer). Approximately 20–25 mg of r*Ph*GshB purified under non–reducing or reducing conditions were obtained from the 500–mL culture of the transformant.

The same procedure was used for the heterologous expression of the *Ph*GshAII gene, even though this enzyme was purified at moment only in absence of β-mercaptoethanol.

2.4 Assay for the activity of r*Ph*GshB and r*Ph*GshA-II

A new assay was set up for measuring the r*Ph*GshB and r*Ph*GshA-II activities, based on the ATP hydrolysis coupled to the GSH synthesis (reaction 2). The ATPase was evaluated as radioactive inorganic phosphate ($^{32}P_i$) released from [γ^{32}P]ATP through the phosphomolybdate method.[31] The reaction was followed kinetically on 50–µl aliquots withdrawn from the reaction mixture at selected times. Unless otherwise indicated, the reaction was carried out in buffer C, supplemented with the substrates glycine and γ–Glu–Cys or cysteine and glutamic acid for r*Ph*GshA-II. The reaction was stopped at 0°C by the addition of an equal volume of 1 M $HClO_4$ supplemented with 5 mM KH_2PO_4 as a $^{32}P_i$ carrier. Following the addition of 300 µl of 20 mM sodium molybdate, phosphate was converted into phosphododecamolybdate complex, which was then extracted by a vigorous stirring for 30 sec with 400 µl isopropylacetate. After a fast spinning to achieve phase separation, 200 µl of the organic phase were counted in 3 mL Emulsifier–Safe (Packard), using the liquid scintillation counter TriCarb 1500 (Packard). The rate constant of the reaction was calculated from the slope of linear kinetics and expressed as mol of $^{32}P_i$ released by one mol r*Ph*GshB/r*Ph*GshA-II in one sec. Blanks for spontaneous [γ^{32}P]ATP hydrolysis determined in the absence of r*Ph*GshB or r*Ph*GshA-II were subtracted.

The kinetic parameters of the ATPase catalysed by r*Ph*GshB, including the K_m values for the three substrates γ–Glu–Cys, glycine and ATP and the V_{max} of the reaction, were derived from Lineweaver–Burk plots of the activity data. To this aim, the concentration of the target substrate was almost equally distributed in the reciprocal *x*–axis around the K_m of the reaction, whereas the concentration of other substrates was essentially saturating. Linearity in double reciprocal plots was evaluated through the squared correlation coefficient, which in almost all cases was higher than 0.98.

The energy of activation E_a and the Arrhenius constant A of the reaction, as well as the related thermodynamic parameters of activation, namely enthalpy (ΔH^*), entropy (ΔS^*) and free energy (ΔG^*), were calculated as reported elsewhere.[32]

2.5 Other methods

Protein concentration was determined by the method of Bradford, using bovine serum albumin as standard.[33] Purity of protein samples was assessed by 12% SDS–PAGE according to standard protocols.[34] The quaternary structure of r*Ph*GshB was evaluated by gel–filtration on a Superdex^{TM} 200 10/300 GL column connected to a FPLC apparatus (GE Healthcare). The mass spectrometry analysis was realised on protein samples desalted by RP–HPLC, as previously reported.[35,36] The number of cysteine residues in r*Ph*GshB was determined by the Ellman assay.[37,38]

RESULTS

3.1 Molecular properties of r*Ph*GshB

The genes encoding GshA and GshB in *P. haloplanktis* have been putatively annotated in the genome of this psychrophilic eubacterium.[25] Two putative genes for *Ph*GshA are present in chromosome I (*Ph*gshA-I; ID 3708000) and II (*Ph*gshA-II; ID 3711501), respectively; vice versa, there is one putative gene for GshB in chromosome I (*Ph*gshB; ID 3708001). In order to characterize the glutathione synthetase activity from a psychrophilic source, a recombinant form of *Ph*GshB (r*Ph*GshB) with the C-terminal lysine replaced by the extrapeptide $LE(H)_6$ was obtained, using the heterologous expression system constituted by the vector v*Ph*GshB, a pET–28a(+) derivative, and the *E. coli* strain BL21(DE3).

The molecular properties of two r*Ph*GshB samples purified in the absence or in the presence of β–mercaptoethanol were assessed by SDS/PAGE analysis (Fig. 1); both were homogenous and their electrophoretic mobility corresponded to a molecular mass of 36 kDa, the expected size for the r*Ph*GshB monomer.

These protein samples were also analysed by ESI/Q-TOF mass spectrometry (Fig. 2). In the absence of β–mercaptoethanol, a single peak was obtained, whose calculated M_r 35888.33 was in agreement with the theoretical value of 35887.03 assigned to the recombinant enzyme, considering the His–tail and the lack of initial methionine.

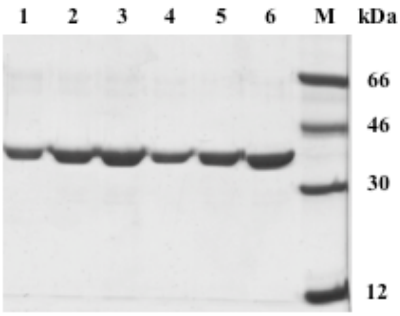

Fig. 1: SDS–PAGE of purified r*Ph*GshB samples. Increasing amounts (2, 4 and 6 µg) of r*Ph*GshB purified in the presence of β–mercaptoethanol (*lanes* 1–3) or in its absence (*lanes* 4–6) were analysed on a 12% polyacrylamide gel. Migration of molecular mass protein standards (*lane* M) is reported on the right.

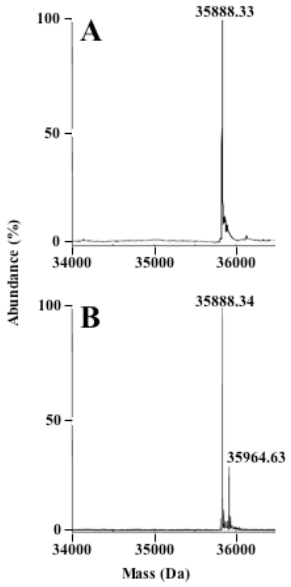

Fig. 2: Mass spectrometry on r*Ph*GshB. Electrospray mass spectrum of a purified r*Ph*GshB sample purified in the absence (*panel **A***) or in the presence of β–mercaptoethanol (*panel **B***). The M_r values of the major peaks are indicated.

Vice versa, in the presence of β–mercaptoethanol, another heavier peak with M_r 35964.63 was found besides the most abundant peak with M_r 35888.34; the extra mass of 76.29 Da could be explained by the formation of a disulfide adduct between a cysteine residue and β–mercaptoethanol, as already demonstrated for the superoxide dismutase from *P. haloplanktis*.[36]

The molecular mass of r*Ph*GshB was also determined by gel filtration chromatography under non–denaturing conditions. Fig. 3 shows the elution profile of different dilutions of the r*Ph*GshB sample purified in the absence of β–mercaptoethanol on a Superdex^{TM} 200 10/300 GL column. Position and broadness of peaks were significantly affected by protein concentration; indeed, after the comparison with protein standards, the extrapolated molecular mass for r*Ph*GshB ranged between 74 and 136 kDa, roughly corresponding to a homodimeric and homotetrameric organization, respectively. Similar profiles were obtained with the r*Ph*GshB sample purified in the presence of β–mercaptoethanol. These data indicate that r*Ph*GshB was probably organised as a homotetramer at high protein concentration on the basis of the elution position of the broad peak observed at the highest concentration of r*Ph*GshB analysed. On the other hand, when the protein concentration was lowered, the homotetramer was unstable and therefore converted to a more stable homodimer, as demonstrated by the elution position of the peak, becoming progressively slower and narrower.

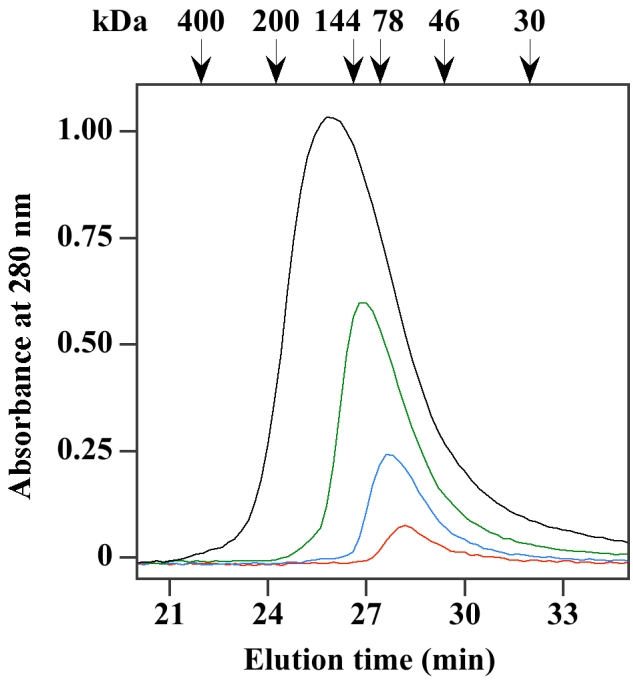

Fig. 3: Gel filtration behaviour of r*Ph*GshB under non–denaturing conditions. The elution profile of a r*Ph*GshB sample purified in the absence of β–mercaptoethanol was analysed on a Superdex^{TM} 200 10/300 GL column. 100 µL of r*Ph*GshB solutions at 0.5 mg mL^{-1} (red line), 1.5 mg mL^{-1} (blue line), 4.0 mg mL^{-1} (green line) or 10.0 mg mL^{-1} (black line) concentration in buffer D were loaded on the column. Elution was realised with buffer D at a flow rate of 0.5 mL min^{-1}. The column was calibrated with six protein standards, namely apoferritin (M_r 400000), β–amylase (M_r 200000), glyceraldehyde–3–phosphate dehydrogenase (M_r 144000), human transferrin (M_r 78000), ovalbumin (M_r 46000) and carbonic anhydrase (M_r 30000); the corresponding elution positions are indicated by arrows on the top. Absorbance was continuously monitored at 280 nm.

Three cysteine residues are present in the amino acid sequence of *Ph*GshB, namely at position 185, 223 and 290 (numbering includes initial methionine). The Ellman assay was used to determine the number of free cysteines in the r*Ph*GshB samples purified in the absence or in the presence of β–mercaptoethanol and the values

found were 2.75 and 2.17, respectively. These data suggest that when r*Ph*GshB was purified in the absence of reducing agents, its three cysteines were present as free sulphidryl groups. The reduced number of free cysteines measured in the protein sample purified in the presence of β–mercaptoethanol reinforces the hypothesis of the formation of an adduct between cysteine(s) and β–mercaptoethanol. However, only part of the protein population harboured this adduct, as also confirmed by the mass spectrometry data and therefore, the covalent modification of the cysteine residue(s) was under-stoichiometric.

3.2 Biochemical properties of r*Ph*GshB

Assays for GshB activity (reaction 2) are usually based on the determination of ADP formed during the GSH synthesis through an indirect enzyme–coupled method. Indeed, the spectrophotometric procedure involves the usage of pyruvate kinase and lactate dehydrogenase to measure ADP formation through NADH oxidation.[39] However, the employment of other enzymes impaired a direct evaluation of the effect of some parameters, such as temperature, pH, ions, on the biochemical properties of the enzyme *Ph*GshB. To this aim, another assay was developed, which directly evaluated the activity of *Ph*GshB through the measurement of the radioactive $^{32}P_i$ released from the radiolabelled [γ^{32}P]ATP. The rate of

$^{32}P_i$ release promoted by r*Ph*GshB in the presence of glycine, γ–Glu–Cys or both compounds is shown in Fig. 4.

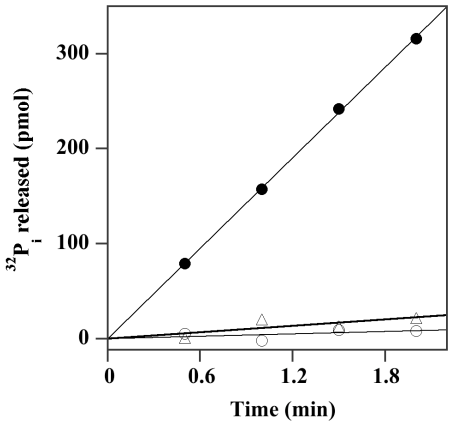

Fig. 4: Time course of ATP hydrolysis by r*Ph*GshB. The reaction mixture contained 0.15 µM r*Ph*GshB, supplemented with 10 mM glycine (○), or 2.5 mM γ–Glu–Cys (△), or both substrates (●), in 250 µl final volume of 100 mM Tris•HCl, pH 7.8 buffer, containing 20 mM $MgCl_2$ and 150 mM KCl. The reaction was carried out at 30°C and started with the addition of 2 mM [γ^{32}P]ATP (specific radioactivity 8.45 cpm $pmol^{-1}$). At the times indicated, aliquots were withdrawn and analysed for the $^{32}P_i$ released, as described in Materials and Methods section.

No significant activity was measured when only one substrate was present in the reaction mixture; vice versa, a well–measurable activity was detected in the presence of both glycine and γ–Glu–Cys. These results indicate that the ATPase catalysed by r*Ph*GshB required the presence of both substrates and was likely coupled to the GSH synthesis. The validity of the new method for measuring the glutathione synthetase activity was demonstrated by the linear dependence of the initial rate of $^{32}P_i$ release with the concentration of r*Ph*GshB, as expected for an enzyme activity (not shown).

The assessment of the biochemical properties possessed by the psychrophilic r*Ph*GshB was first carried out with the enzyme sample purified in the absence of β–mercaptoethanol, to avoid any interference by an understoichiometric thiolic adduct on the enzyme. To establish the best experimental conditions for measuring the ATPase activity triggered by r*Ph*GshB, its pH and ionic dependence was investigated (Fig. 5). To study the effect of pH, the chosen buffers, Tris HCl and imidazole HCl supplemented with 5 mM $MgCl_2$ and 150 mM KCl, covered the 6.0 – 8.6 pH range. As shown in Fig. 5A, the activity was affected by both pH and type of buffer. Maximum levels of activity were reached with the Tris HCl buffer in the 7.4 – 8.6 pH range. For this reason, the following experiments were all carried out in 20 mM Tris HCl buffer, pH 7.8. The ionic dependence of the r*Ph*GshB activity was focused on the assessment of the eventual specific requirement for monovalent and/or divalent cations. Concerning the investigation on divalent cations, the buffer employed contained 150 mM KCl and an increasing concentration of chlorides of Mg^{++} or Mn^{++} (Fig. 5B). The presence of a divalent cation was absolutely required for the activity and Mg^{++} was significantly more effective than Mn^{++}. Indeed, maximum activity was reached in the presence of 5 mM $MgCl_2$ and a further addition of this salt caused a little decrease of activity. A narrow bell–shaped curve was instead observed when the effect of $MnCl_2$ was analysed, and the best condition for the Mn–dependent activity was found in the

presence of 0.8 mM $MnCl_2$. In the study related to monovalent cations, the buffer employed contained 5 mM $MgCl_2$ and an increasing concentration of chlorides of the most common monovalent cations, namely Na^+ or K^+ (Fig. 5C).

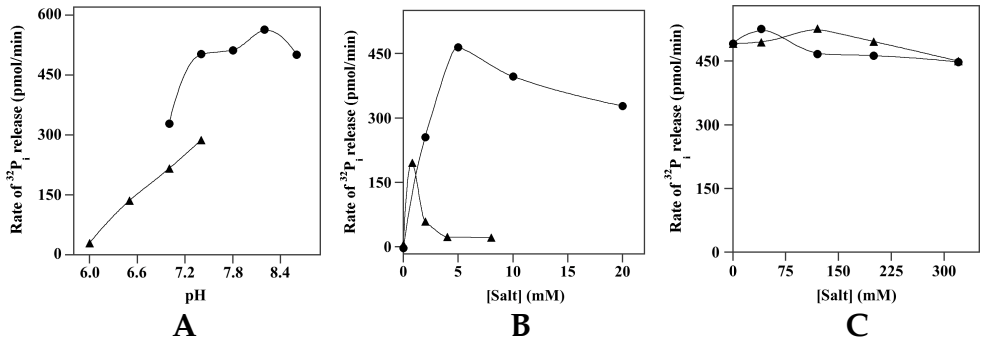

Fig. 5: pH and ionic dependence of the ATPase activity catalysed by r*Ph*GshB. (***A***) Effect of pH. The reaction mixture contained 0.17 µM r*Ph*GshB, 10 mM glycine and 2.5 mM γ–Glu–Cys in 250 µl final volume of 100 mM Tris•HCl (●) or 100 mM imidazole•HCl buffer (▲), at the pH indicated, supplemented with 5 mM $MgCl_2$ and 150 mM KCl. (***B***) Effect of divalent cations. The reaction mixture contained the same concentrations of r*Ph*GshB, glycine and γ–Glu–Cys as in ***A***, in 250 µl final volume of 100 mM Tris•HCl, pH 7.8 buffer, supplemented with 150 mM KCl and the indicated concentrations of $MgCl_2$ (●) or $MnCl_2$ (▲). (***C***) Effect of monovalent cations. The reaction mixture contained the same concentrations of r*Ph*GshB, glycine and γ–Glu–Cys as in ***A***, in 250 µl final volume of 100 mM Tris•HCl, pH 7.8 buffer supplemented with 5 mM $MgCl_2$ and the indicated concentrations of KCl (●) or NaCl (▲). All reactions were carried out at 15°C, started with the addition of 2 mM [γ^{32}P]ATP (specific radioactivity 1.27 – 2.19 cpm $pmol^{-1}$) and were followed kinetically. To this aim, aliquots were withdrawn at selected times and analysed for $^{32}P_i$ released. The data were expressed as rate of $^{32}P_i$ release, as evaluated from the slope of linear kinetics.

An almost maximum level of activity was reached in the absence of these salts, thus indicating that r*Ph*GshB did not require the presence of monovalent cations for its activity. Moreover, no significant variation of this level of activity was observed in the

presence of the indicated concentrations of NaCl or KCl. Therefore, the ATPase sustained by r*Ph*GshB absolutely required a divalent cation, whereas the presence of a monovalent cation was dispensable.

The affinity of r*Ph*GshB for its three substrates, γ–Glu–Cys, glycine and ATP was evaluated at 15°C, the optimum growth temperature of *P. haloplanktis*.[40]

To this aim, the effect of various concentrations of each substrate on the activity was determined in the presence of saturating concentrations of the other substrates. The resulting Lineweaver–Burk plot shows that an almost identical value of maximum rate of ATP hydrolysis (V_{max}) was extrapolated from the three straight lines (Fig. 6), thus proving that in the three different conditions the reaction depended on a single substrate. In particular, the value of k_{cat} calculated from the extrapolated V_{max} was 1.85, 1.93 and 2.03 s^{-1} for the steady–state measurement depending on ATP, γ–Glu–Cys and glycine, respectively.

Concerning the affinity for the different substrates, the values of K_m for ATP and γ–Glu–Cys were quite similar (0.26 and 0.25 mM, respectively), whereas a slightly higher K_m (0.75 mM) was determined for glycine. These data prove that the psychrophilic r*Ph*GshB was endowed with a significant catalytic efficiency at 15°C, as evaluated through the k_{cat}/K_m ratios.

It has been reported that GSSG, the oxidized form of glutatione, is an inhibitor of GshB from *E. coli*.[41] To this aim, the effect of

increasing GSSG concentrations on the ATPase activity by r*Ph*GshB was investigated. As shown in Fig. 7, a dose-dependent decrease of activity was observed and r*Ph*GshB was almost completely inhibited by 24 mM GSSG.

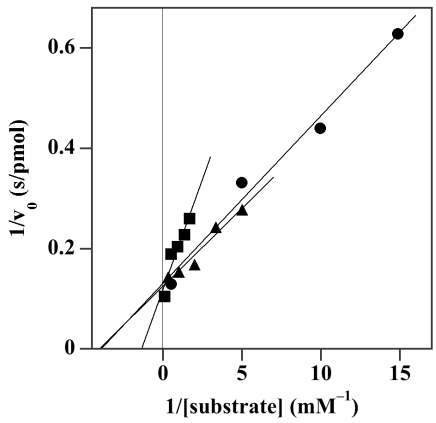

Fig. 6: Lineweaver–Burk plot of the ATPase of r*Ph*GshB for evaluating the kinetic parameters of the substrates ATP, glycine and γ–Glu–Cys. The reaction mixture for measuring the kinetic parameters of ATP contained 0.17 µM r*Ph*GshB, 10 mM glycine and 2.5 mM γ–Glu–Cys in 250 µl final volume of buffer C. In this experimental condition the reaction started with the addition of the indicated concentrations of [γ^{32}P]ATP (●) (specific radioactivity 3.98 – 166.4 cpm pmol^{-1}). For measuring the kinetic parameters of glycine or γ–Glu–Cys, the reaction mixture contained the same concentration of r*Ph*GshB, 2.5 mM γ–Glu–Cys and the indicated concentration of glycine (■), or 10 mM glycine and the indicated concentration of γ–Glu–Cys (▲), in 250 µl final volume of buffer C, respectively. In these two experimental conditions the reaction started with the addition of 2 mM [γ^{32}P]ATP (specific radioactivity 3.08 cpm pmol^{-1}). All reactions were carried out at 15°C and followed kinetically, by analysing the amount of $^{32}P_i$ released on aliquots withdrawn at appropriate times. The values of v_0 (pmol ATP hydrolysed s^{-1}) were calculated from the slope of linear kinetics.

In order to study the cold adaptation of r*Ph*GshB, its psychrophilic behaviour was analysed through the effect of temperature on the activity and stability of the enzyme. The thermo–dependence of the

r*Ph*GshB activity was analysed through the determination of the kinetic parameters related to the affinity for ATP in the temperature interval 10 – 30°C. As reported in Table 1, the enzyme was active even at 10°C, a further prove of its cold adaptation; however, above 10°C, a significant enhancement of the activity with temperature was observed.

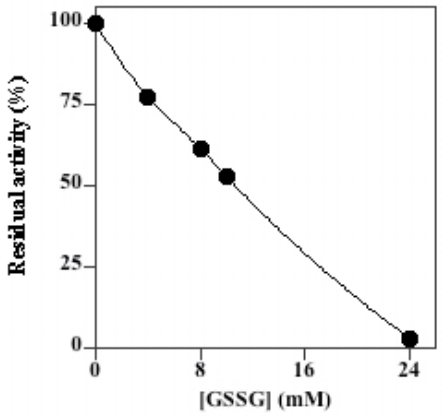

Fig. 7: Inhibition profile of r*Ph*GshB by GSSG. The reaction mixture contained 0.17 µM r*Ph*GshB, 10 mM glycine, 2.5 mM γ–Glu–Cys and the indicated concentrations of GSSG in 250 µl final volume of buffer C. The residual ATPase activity was measured at 15°C essentially as reported in Fig. 5 (specific radioactivity of [γ^{32}P]ATP 1.11 cpm pmol^{-1}). The residual ATPase of the treated samples was expressed as a percentage of an untreated control kept at 0°C.

On the other hand, the effect of temperature on K_m for ATP was negligible, because the corresponding values ranged between 0.17 and 0.28 mM in the 10 – 30°C interval. These data indicate that the catalytic efficiency of r*Ph*GshB, evaluated through the k_{cat}/K_m ratio, significantly increased with temperature; for instance, a 3.3–fold enhancement of this ratio was calculated between 10 and 25°C. The

thermophilicity of r*Ph*GshB was also evaluated through the Arrhenius plot of the k_{cat} values (Fig. 8).

Table 1: Effect of temperature on the kinetic parameters of the ATPase activity of r*Ph*GshB

Temperature (°C)	k_0 (s^{-1})	K_m for ATP (mM)	k_0/K_m (s^{-1}•mM^{-1})
10	0.87	0.17	5.1
15	1.85	0.26	7.1
20	2.42	0.18	13.4
25	4.72	0.28	16.9
28	4.99	0.21	23.8
30	5.32	0.18	29.6

Values of k_{cat} and K_m for ATP were calculated from Lineweaver–Burk plots realised on experiments carried out at the indicated temperatures as described in Fig. 6.

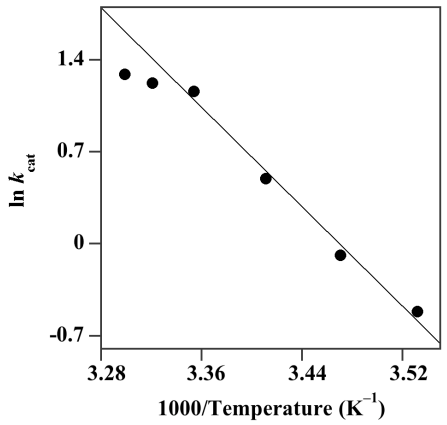

Fig. 8: Arrhenius plot of the ATPase activity triggered by r*Ph*GshB. The k_{cat} values reported in Table 1 were analyzed according to the Arrhenius equation. A linear fit of the data was obtained in the 10 – 25°C temperature interval.

The plot was linear in the 10 – 25°C interval and the calculated energy of activation (E_a) was 75.0 kJ/mol, a value unusually high for a psychrophilic enzyme. The other thermodynamic parameters of the ATPase reaction, calculated at 15°C, are reported in Table 2.

Table 2: Energy of activation and other thermodynamic parameters of the ATPase activity of r*Ph*GshB

E_a	ΔH^{*} [a]	ΔS^{*} [a]	ΔG^{*} [a]
kJ mol^{-1}	kJ mol^{-1}	J mol^{-1} K^{-1}	kJ mol^{-1}
75.0	72.6	11.3	69.3

The energy of activation and the Arrhenius constant were derived from the experiment reported in Fig. 7.

[a]Calculated at 15 °C.

The thermal stability of r*Ph*GshB was investigated through a heat inactivation profile. To this aim, aliquots of an enzyme sample were incubated for 10 min at different temperatures and then immediately cooled on ice. The residual ATPase activity of the treated samples was reported as a function of temperature (Fig. 9). Under these conditions the calculated temperature for the half–inactivation ($T_{1/2}$) of r*Ph*GshB was 50.5°C, a value moderately high for a psychrophilic enzyme, although not unusual for antioxidant macromolecules. The heat stability of r*Ph*GshB was also investigated through inactivation kinetics realised at temperatures ranging between 45°C and 54°C.

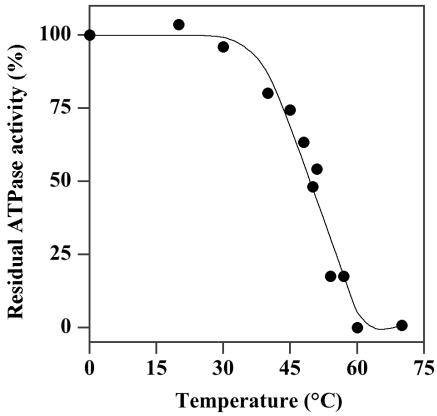

Fig. 9: Heat inactivation profile of r*Ph*GshB. A 1.0 µM solution of r*Ph*GshB in 20 mM Tris•HCl, pH 7.8 buffer, was incubated for 10 min at the indicated temperatures. After an ice–chilling for 30 min, the ATPase activity was measured at 15°C in buffer C essentially as reported in Fig. 5 (specific radioactivity of [γ^{32}P]ATP 3.30 cpm pmol^{-1}). The residual ATPase of the treated samples was expressed as a percentage of an untreated control kept at 0°C.

The heat inactivation of the enzyme followed first–order kinetics at each temperature and the corresponding inactivation rate constants (k_{in}) were treated according to the Arrhenius equation (Fig. 10).

A linear plot was in the chosen interval of temperature allowed the determination of the energetic parameters of the heat inactivation process. The values of E_a, ΔH^*, ΔS^*, and ΔG^* are reported in Table 3. In particular, the value of E_a was 208 kJ/mol, as usually found for psychrophilic enzymes.

3.3 Crystallization of r*Ph*GshB

r*Ph*GshB was successfully crystallized using vapor-diffusion and small-scale batch (microbatch) methods. Initial screenings using

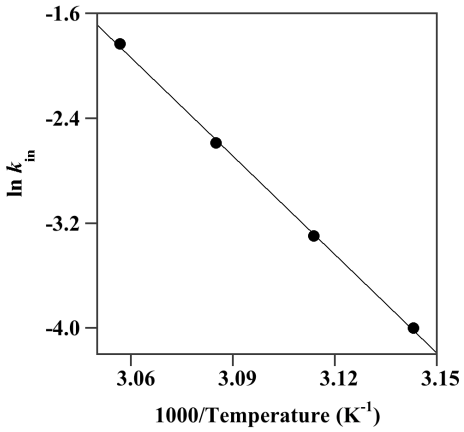

Fig. 10: Arrhenius plot of the heat inactivation process of r*Ph*GshB. The k_{in} values were obtained from inactivation kinetics of a 1.0 μM solution of r*Ph*GshB in 20 mM Tris•HCl, pH 7.8 buffer, at 45, 48, 51 or 54°C. At selected times aliquots were withdrawn from each incubation and immediately chilled on ice for 30 min. The residual ATPase activity was measured at 15°C in buffer C essentially as reported in Fig. 5 (specific radioactivity of [γ^{32}P]ATP 1.97 – 3.06 cpm pmol^{-1}). The data were analyzed according to a first–order kinetics to obtain the rate constant of heat inactivation (k_{in}), which were then treated according to the Arrhenius equation.

Table 3: Activation energetic parameters of the heat inactivation process of r*Ph*GshB

E_a	ΔH^{*} [a]	ΔS^{*} [a]	ΔG^{*} [a]
kJ mol^{-1}	kJ mol^{-1}	J mol^{-1} K^{-1}	kJ mol^{-1}
208.0	205.2	366.2	86.9

The energy of activation and the Arrhenius constant were derived from the experiment reported in Fig. 10.

[a]Calculated at 50 °C.

commercially available solutions (Crystal Screen kits I and II, and Index kits from Hampton Research, Laguna Niguel, USA, www.hamptonreaserch.com) revealed several promising conditions for the crystallization of r*Ph*GshB. All favourable conditions were characterized by the presence of polyethylene glycol as precipitating agent.

Crystallization trials using vapor diffusion method produced small and bad-diffracting crystals. Preliminary X-ray diffraction data, in fact, showed that cubic crystals are intrinsically disordered and that the largest rod-like crystals obtained by vapor diffusion diffract at most at 3.5 Å resolution; the crystals belong to the space group $P2_12_12_1$, with unit-cell parameters a = 82.81 Å, b = 119.94 Å, c = 159.32 Å.

Further optimization of the crystallization conditions to grow larger and thicker crystals suitable for diffraction data collection at high resolution were performed using the microbatch method. This procedure consists of slowly and thoroughly mixing the precipitant with the protein and then placing the mixture in a well-sealed container. Usually the drop is incubated under silicon oil to prevent too rapid dehydration.[42] The benefits of microbatch have been well documented.[42,43] In the present case, a modified microbatch method, defined without-oil microbatch, has been used: the drop is stored in the presence of a reservoir with the same precipitant concentration, to avoid drop evaporation.[44] The crystals obtained with this procedure diffract to

2.34 Å resolution and are isomorphous to those obtained by hanging drop experiments, with unit-cell parameters a = 83.28 Å, b = 119.88 Å, c = 159.82 Å (Fig. 11 and Table 4). Matthews coefficient calculations suggested the presence of four chains of r*Ph*GshB (V_M = 2.79 Å^3 Da^{-1}, 56% solvent content) in the asymmetric unit. The application of the molecular replacement allowed the identification of orientation and position of the four chains in the asymmetric unit that gave a satisfactory fit of the experimental data. Rebuilding and refinement of the whole structure is in progress. Calculated preliminary (*F*o-*F*c) and (2*F*o-*F*c) difference Fourier maps are of excellent quality.

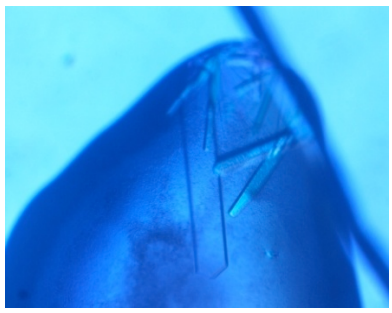

Fig. 11: Image of crystals grown by without–oil microbatch technique

Initial studies on three-dimensional structure of r*Ph*GshB are in progress. The asymmetric unit contains four subunits arranged as a tetramer. Two subunits are in close contact and form a dimer, whereas two dimers form a tetramer with two solvent regions. The structure of each subunit is composed of three domains: N- terminal, central and C-terminal domains. The ATP-binding site is located in

the cleft between the central and C-terminal domains. The active site is a deep cleft lined by peptide segments 86-89, 203-208, 273-275 and 283-289. This region is able to accommodate the γ–Glu–Cys and the ATP molecules. Most of the active site residues are well defined in electron density maps.

Table 4. Data collection statistics on r*Ph*GshB crystals

Space group	$P2_12_12_1$
Cell parameters:	
a (Å)	83.28
b (Å)	119.88
c (Å)	159.82
Resolution limits (Å)	50.00–2.34
Highest resolution shell (Å)	2.45–2.34
No. of observations	337677
No. of unique reflections	66744
Completeness (%)	97.1 (85.0)
I/s (I)	20.5 (2.6)
Average multiplicity	5.1 (2.5)
R_{merge} (%)	11.5 (40.5)
R_{pim}	5.0 (27.5)
R_{rim}	12.7 (49.6)
Mosaicity	0.3

Values in parentheses correspond to the highest resolution shells.

3.4 Purification and preliminary characterization of r*Ph*GshA-II

A recombinant form of *Ph*GshA-II was obtained to start the study on the biochemical properties of this enzyme. The new assay method used for the characterization of r*Ph*GshB was valid also for the characterization of r*Ph*GshA-II (Fig. 12). Indeed, as shown in Fig. 12A, the ATPase activity required the presence of the specific substrates of *Ph*GshA, namely glutamate and cysteine. Therefore, it is

likely that the ATPase activity of *Ph*GshA-II is coupled to the synthesis of γ–Glu–Cys.

The sample of r*Ph*GshA-II used for its initial characterization was purified in the absence of β–mercaptoethanol. However, as shown in Fig. 12B, the ATPase activity of r*Ph*GshA-II required for its maximal level the presence in the reaction mixture of a reducing agent, such as DTT. This behaviour could indicate that the reduced form of one or more cysteine residues is essential for the enzyme activity.

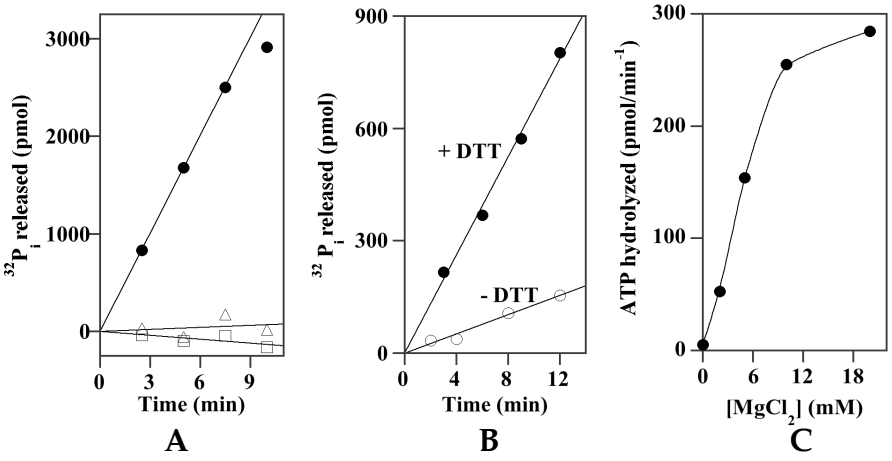

Fig. 12: ATPase activity of r*Ph*GshA-II. (***A***) Requirement of substrates. The reaction mixture contained 0.61 µM r*Ph*GshA-II, supplemented with 10 mM glutamate (□), or 2.5 mM cysteine (△), or both substrates (●), in 250 µl final volume of buffer C supplemented with 1 mM DTT. (***B***) Effect of the reducing agent DTT. The reaction mixture contained 0.08 µM r*Ph*GshA-II, 10 mM glutamate and 2.5 mM cysteine, in 250 µl final volume of buffer C without (○) or with 1 mM DTT (●). (***C***) Effect of the cation Mg^{++}. The reaction mixture contained 0.31 µM r*Ph*GshA-II, 10 mM glutamate and 2.5 mM cysteine in 250 µl final volume of 100 mM Tris•HCl, pH 7.8 buffer, supplemented with 150 mM KCl, 1 mM DTT and the indicated concentrations of $MgCl_2$. All reactions were carried out at 15°C, started with the addition of 2 mM [γ^{32}P]ATP (specific radioactivity 0.17 – 0.51 cpm pmol^{-1}) and were followed kinetically. To this aim, aliquots were withdrawn at selected times and analysed for $^{32}P_i$ released. In panel ***C*** the rate of ATP hydrolysis was calculated from the slope of linear kinetics.

Finally, the requirement of the divalent cation Mg^{++} for the r*Ph*GshA-II activity was assessed (Fig. 12C). Interestingly, significantly higher concentrations (10-20 mM) of of this cation were needed, compared to those established for r*Ph*GshB (5 mM). Furthermore, the replacement of Mg^{++} by Mn^{++} was unseccesful for the detection of activity (not shown).

DISCUSSION

The psychrophile *P. haloplanktis* was chosen as a model source for an investigation on the enzyme mechanism leading to the GSH synthesis in cold–adapted microorganisms. Indeed, the presence of GSH in this source was hypothesized on the basis of the covalent modification caused by the oxidized form of this thiol on some antioxidant enzymes from this psychrophile.[26,27] In the case of superoxide dismutase from *P. haloplanktis*, the modified enzyme became more resistant to its physiological inactivator peroxynitrite; furthermore, glutathionylated proteins were detected even in a growing culture of *P. haloplanktis* and the extent of modification increased under oxidative growth conditions.[26] Therefore, it is likely that GSH exerts its control in the redox homeostasis of *P. haloplanktis*, as emerging from most gram–negative gamma–proteobacteria.[10]

This work presented in this thesis deals with the characterization of the enzyme system aimed at the GSH synthesis in *P. haloplanktis*. As usually observed in other gamma–proteobacteria, two distinct activities are required to synthesize GSH. The main focus of this investigation was on the enzyme *Ph*GshB, converting γ–Glu–Cys and glycine into GSH. However, an initial characterization of the first enzyme involved in the GSH biosynthesis, *Ph*GshA-II, converting glutamate and cysteine into γ–Glu–Cys, is also presented.

A recombinant form of *Ph*GshB was purified and characterised. The investigation on the molecular properties of r*Ph*GshB was carried out on protein samples purified under non–reducing or reducing conditions. Interestingly, the mass spectrometry data and the number of free cysteine residues determined by the Ellman assay suggested the presence of a reactive cysteine in r*Ph*GshB, which underwent a covalent modification by β–mercaptoethanol, when the enzyme sample was purified in the presence of this reducing agent. The reactivity towards β–mercaptoethanol was already demonstrated for another anti–oxidant enzyme, superoxide dismutase, from *P. haloplanktis*.[36] The presence of cysteines, targets of covalent modification by cellular thiols in enzymes involved in the control of oxidative metabolism of *P. haloplanktis*, could be relevant for the cold adaptation of this source.

The structural organization of r*Ph*GshB was analysed by gel filtration chromatography under non–denaturing conditions. On the basis of the comparison of the elution profiles obtained at different protein concentration, r*Ph*GshB could be organised as a homotetramer or a homodimer at high or low protein concentration, respectively. This behaviour could suggest that the assemblage of the homotetramer involved a two–step process. In the first step strong interactions should lead to a stable homodimer, whereas in the second step weak interactions could allow the assemblage of two homodimers into a homotetramer. Indeed, when the protein

concentration was progressively lowered at room temperature, the homotetramer was converted into the more stable homodimer. The crystallization data indicated that r*Ph*GshB is structuraly organised as a homotetramer. This finding confirms our hypothesis that r*Ph*GshB forms a tetramer at high proytein concentration, as usually occurred during crystal growing. Furthermore, it has been reported that the corresponding GshB from *E. coli* is organised as a stable homotetramer.[45–47] We cannot exclude that the postulated less stable homotetramer in r*Ph*GshB be more stable at the working temperature of *P. haloplanktis*. A more detailed and temperature–dependent structural analysis is required to address this point.

The study on the functional properties of r*Ph*GshB was faced with a convenient assay system, which measured the activity of the psychrophilic enzyme in the absence of other enzymes, such as lactate dehydrogenase and pyruvate kinase. To this aim a new method was set up, which involved the direct measurement of the ATP hydrolysis promoted by r*Ph*GshB; only this approach could lead to the relevant information on the cold–adaptation of the enzyme in terms of thermophilicity and thermostability. The results showed that the ATPase catalysed by r*Ph*GshB required the presence of both substrates, glycine and γ–Glu–Cys. This finding clearly suggested that the activity was likely coupled to the GSH synthesis; therefore the assay could represent a valid tool to measure the glutathione synthetase activity of purified samples of GshB. The best ionic

conditions (pH and salts) for the assay were then investigated. The pH optimum for the ATPase catalysed by r*Ph*GshB ranged between 7.5 and 7.8, a value not far away from that reported for the corresponding enzyme from *E. coli*.[41,47] Concerning the ionic requirement for the activity, the psychrophilic enzyme absolutely needed a divalent cation, such as Mg^{2+} or Mn^{2+}, a feature typical for ATP hydrolysing enzymes and observed also in *Ec*GshB.[41] Among the two cations, Mg^{2+} was 2.4–fold more effective than Mn^{2+} at the respective optimal concentration; moreover, at over–optimal concentration, the stimulation by Mn^{2+} was quickly reverted, whereas only a minimum decrease of activity was observed with Mg^{2+}. Concerning the effect of monovalent cations, the results proved that cations such as Na^{+} or K^{+} were dispensable for the activity. Therefore, the presence of monovalent cations required for other enzymes isolated from *P. haloplanktis*, such as α–amylase[48] or polynucleotide phosphorylase,[49] was not extended to r*Ph*GshB.

In the GSH synthesis catalysed by GshB, the enzyme interacts with three substrates, γ–Glu–Cys, glycine and ATP. It has been proposed that the mechanism for this reaction involves phosphorylation of the C–terminal carboxylate of γ–Glu–Cys by γ–phosphate of ATP, and the following nucleophilic attack of glycine on the acyl phosphate intermediate to form GSH and ADP.[45–47, 50] The determination of the steady–state kinetic parameters of r*Ph*GshB at 15°C proves that the psychrophilic enzyme was endowed with a

significant catalytic efficiency at the optimum growth temperature of *P. haloplanktis*. For instance, the calculated k_{cat}/K_m referred to the steady–state measurement depending on the substrate ATP was 7.1 s^{-1} mM^{-1}, a value in the range of those reported for the corresponding enzyme from other sources at the respective working temperatures.[50–53] The affinity of r*Ph*GshB for its three substrates was evaluated through the K_m values: the enzyme showed a slightly lower affinity for glycine compared to γ–Glu–Cys or ATP. The K_m values of r*P h*GshB were also compared with those reported for the corresponding enzyme from other sources (Table 5). A noticeable similarity was found with the data from the mesophile *E. coli*[50] or the small eukaryote *S. pombe*,[51] including the slightly lower affinity for glycine. In higher eukaryotes, such as *A. thaliana*[52] or humans[53], an improvement of the affinity for ATP and a small reduction of that for glycine made more evident the different affinities among these substrates. A similar finding with an improvement in the affinity for γ–Glu–Cys was found at least in *A. thaliana*.

Table 5: Affinity of GshB for its substrates in various sources

Source	K_m (mM)			Reference
	ATP	γ–Glu–Cys	Gly	
Pseudoalteromonas haloplanktis	0.26	0.25	0.75	This thesis
Escherichia coli	0.24	0.24	0.91	50
Schizosaccharomyces pombe	0.45	0.27	0.67	51
Arabidopsis thaliana	0.057	0.039	1.51	52
Homo sapiens	0.07	0.66 [a]	1.75	53

[a] Measured with γ–glutamyl–α–aminobutyrate, an analogue of γ–Glu–Cys.

An investigation on the thermophilicity and thermostability of r*Ph*GshB was carried out, thanks to the direct assay for measuring the enzyme activity. Concerning the effect of temperature on its coupled ATPase, r*Ph*GshB was endowed with a significant activity already at 10°C, thus confirming its cold–adaptation; however, the rate of ATP hydrolysis underwent a significant improvement in the temperature range 10 – 25°C and then remained approximately unchanged between 25 and 30°C. On the other hand, the affinity of r*Ph*GshB for ATP was essentially unchanged in the whole 10 – 30°C interval. The discrete thermophilicity of r*Ph*GshB is somehow atypical, because cold–adaptation of psychrophilic enzymes is based on their full activity at low temperatures, whereas thermophilicity is dispensable. On the other hand, a similar discrete thermophilicity was reported for another enzyme involved in the redox balance of *P. haloplanktis*, such as thioredoxin.[38] The high value of E_a calculated for the ATPase reaction confirmed the high thermophilicity of the psychrophilic enzyme. Moreover, the other thermodynamic parameters of this reaction involved a high enthalpic barrier and a low entropic factor.

The observed lack of a significant improvement of ATPase activity above 25°C prompted an evaluation on the heat stability of r*Ph*GshB. The higher value of $T_{1/2}$, well above 25°C, extrapolated form the heat inactivation profile of r*Ph*GshB indicated that the enzyme was endowed with a discrete heat resistance. Therefore, other explanations must be invoked for the topping up reached at 25°C in

the thermodependence of r*Ph*GshB. For instance, r*Ph*GshB could be endowed with a lower heat resistance, when exploiting its catalytic action at the selected temperature. Indeed, when measuring its thermodependence, r*Ph*GshB interacted with three substrates during the multifactorial experimental conditions used for the assay. Another possible explanation resides in the postulated conversion of an active homotetramer into a less active homodimer, a process eventually more evident at temperatures higher than 25°C. The moderate heat resistance of the psychrophilic enzyme was further investigated with the determination of the energetic parameters of the heat inactivation process. The calculated E_a was in the range of the values found in typical psychrophilic enzymes; concerning the other thermodynamic parameters, the low enthalpic barrier was accompanied to a significantly favourable entropic process, thus confirming the psychrophlic behaviour of the enzyme, in spite of its discrete heat resistance.

Crystals of r*Ph*GshB adapted for the resolution of the 3D-structure of the first psychrophilic glutathione synthetase were also obtained thanks to the without-oil microbatch method. The X-ray diffraction data were already collected and the phase problem solved. The preliminary data on the crystal structure of r*Ph*GshB allowed an investigation on its structural organization and the identification of the three domains in the subunit; furthermore, some information was obtained on the binding sites of r*PhG*shB for its substrates. When the

resolution of the 3D-structure of r*Ph*GshB will be completed, it will be possible to carry out a detailed comparison of its structure with that of the related protein from *E. coli*, in order to analyse the flexibility of both enzymes by using thermal B-factor distributions.

Conclusion

The characterization of a psychrophilic glutathione synthetase represents the first approach on the study of the biosynthesis of GSH in cold–adapted microorganisms. Another enzyme, glutamyl–cysteine ligase, participates to this relevant process and therefore future research will be devoted to the characterization of this activity in *P. haloplanktis*; indeed the reconstitution of the enzyme system for GSH synthesis in *P. haloplanktis* is an essential tool in studies concerning the possible regulation of growth and survival of this microorganism by GSH.

REFERENCES

1. A. Meister and M. E. Anderson, Glutathione, *Annu. Rev. Biochem.*, 1983, 52, 711–760.
2. R. C. Fahey, G. L. Newton, B. Arrick, T. Overdank-Bogart and S. B. Aley, *Entamoeba histolytica*: a eukaryote without glutathione metabolism, *Science*, 1984, 224, 70–72.
3. M. J. May, T. Vernoux, C. Leaver, M. Van Montagu and D. Inzé, Glutathione homeostasis in plants: implications for environmental sensing and plant development, *J. Exp. Bot.*, 1998, 49, 649–667.
4. M. E. Anderson, Glutathione: an overview of biosynthesis and modulation, *Chem. Biol. Interact.*, 1998, 111–112, 1–14.
5. I. Rahaman and W. MacNee, Oxidative stress and regulation of glutathione in lung inflammation, *Eur. Respir. J.*, 2000, 16, 534–554.
6. R. C. Fahey, W. C. Brown, W. B. Adams and M. B. Worsham, Occurrence of glutathione in bacteria, *J. Bacteriol.*, 1978, 133, 1126–1129.
7. R. C. Fahey and A.R. Sundquist, Evolution of glutathione metabolism, *Adv. Enzymol. Relat. Areas Mol. Biol.*, 1991, 64, 1–53.
8. M. J. Penninckx and M. T. Elskens, Metabolism and functions of glutathione in micro-organisms, *Adv. Microb. Physiol.*, 1993, 34, 239–301.
9. G. L. Newton, K. Arnold, M. S. Price, C. Sherrill, S. B. Delcardayre, Y. Aharonowitz, G. Cohen, J. Davies, R. C. Fahey and C. Davis, Distribution of thiols in microorganisms: mycothiol is a major thiol in most actinomycetes, *J. Bacteriol.*, 1996, 178, 1990–1995.
10. L. Masip, K. Veeravalli and G. Georgiou, The many faces of glutathione in bacteria, *Antioxid. Redox Signal.*, 2006, 8, 753–762.
11. J. A.Thomas, B. Poland and R. Honzatko, Protein sulfhydryls and their role in the antioxidant function of protein S-thiolation, *Arch. Biochem. Biophys.*, 1995, 319, 1–9.

12. P. Klatt and S. Lamas, Regulation of protein function by S-glutathiolation in response to oxitative and nitrosative stress, *Eur. J. Biochem.*, 2000, 267, 4928–4944.
13. I. Dalle Donne, R. Rossi, G. Colombo, D. Giustarini and A. Milzani, Protein S-glutathionylation: a regulatory device from bacteria to humans, *Trends Biochem. Sci.*, 2009, 34, 85–96.
14. B. E. Janowiak and O. W. Griffith, Glutathione synthesis in *Streptococcus agalactiae*. One protein accounts for γ-glutamylcysteine synthetase and glutathione synthetase activities, *J. Biol. Chem.*, 2005, 280, 11829–11839.
15. S. Gopal, I. Borovok, A. Ofer, M. Yanku, G. Cohen,W. Goebel, J. Kreft and Y. Aharonowitz, A multidomain fusion protein in *Listeria monocytogenes* catalyzes the two primary activities for glutathione biosynthesis, *J. Bacteriol.*, 2005, 187, 3839–3847.
16. B. Vergauwen, D. De Vos and J. J. Van Beeumen, Characterization of the bifunctional γ-glutamate-cysteine ligase/glutathione synthetase (GshF) of *Pasteurella multocida*, *J. Biol. Chem.*, 2006, 281, 4380–4394.
17. O. W. Griffith and R. T. Mulcahy, The enzymes of glutathione synthesis: γ-glutamylcysteine synthetase, *Adv. Enzymol. Relat. Areas Mol. Biol.*, 1999, 73, 209–267.
18. P. G. Richman and A. Meister, Regulation of γ-glutamyl-cysteine synthetase by nonallosteric feedback inhibition by glutathione, *J. Biol. Chem.*, 1975, 250, 1422–1426.
19. S. R. Soltaninassab, K. R. Sekhar, M. J. Meredith and M. L. Freeman, Multi-faceted regulation of γ-glutamylcysteine synthetase, *J. Cell. Physiol.*, 2000, 182, 163–170.
20. J. J. Abbott, J. Pei, J. L. Ford, Y. Qi, V. N. Grishin, L. A. Pitcher, M. A. Phillips and N. V. Grishin, Structure prediction and active site analysis of the metal binding determinants in γ-glutamylcysteine synthetase, *J. Biol. Chem.*, 2001, 276, 42099–42107.
21. B. S. Kelly, W. E. Antholine and O. W. Griffith, *Escherichia coli* γ-glutamylcysteine synthetase. Two active site metal ions affect substrate and inhibitor binding, *J. Biol. Chem.*, 2002, 277, 50–58.

22. J. A. Chesney, J. W. Eaton and J. R. Mahoney Jr, Bacterial glutathione: a sacrificial defense against chlorine compounds, *J. Bacteriol.*, 1996, 178, 2131–2135.
23. J. T. Greenberg and B. Demple, Glutathione in *Escherichia coli* is dispensable for resistance to H_2O_2 and γ-radiation, *J. Bacteriol.*, 1986, 168, 1026–1029.
24. C. Sherrill and R. C. Fahey, Import and metabolism of glutathione by *Streptococcus mutans*, *J. Bacteriol.*, 1998, 180, 1454–1459.
25. C. Medigue, E. Krin, G. Pascal, V. Barbe, A. Bernsel, P. N. Bertin, F. Cheung, S. Cruveiller, S. D'Amico, A. Duilio, G. Fang, G. Feller, C. Ho, S. Mangenot, G. Marino, J. Nilsson, E. Parrilli, E. P. Rocha, Z. Rouy A. Sekowska, M. L. Tutino, D. Vallenet, G. von Heijne and A. Danchin, Coping with cold: the genome of the versatile marine Antarctica bacterium *Pseudoalteromonas haloplanktis* TAC125, *Genome Res.*, 2005, 15, 1325–1335.
26. I. Castellano, M. R. Ruocco, F. Cecere, A. Di Maro, A. Chambery, A. Michniewicz, G. Parlato, M. Masullo and E. De Vendittis, Glutathionylation of the iron superoxide dismutase from the psychrophilic eubacterium *Pseudoalteromonas haloplanktis*, *Biochim. Biophys. Acta*, 2008, 1784, 816–826.
27. P. Falasca, G. Evangelista, R. Cotugno, S. Marco, M. Masullo, E. De Vendittis and G. Raimo, unpublished communication
28 M. Masullo, P. Arcari, B. de Paola, A. Parmeggiani and V. Bocchini, Psychrophilic elongation factor Tu from the Antarctic *Moraxella* sp. TAC II 25: biochemical characterization and cloning of the encoding gene. *Biochemistry*, 2000, 39, 15531–15539.
29 J. Sambrook, E. F. Fritsch and T. Maniatis, *Molecular cloning: a laboratory manual*, 2nd ed. Cold Spring Harbor Laboratory Press, Cold Spring Harbor, NY, 1989.
30. A. Merlino, I. Russo Krauss, A. Albino, A. Pica, A. Vergara, M. Masullo, E. De Vendittis and F. Sica, Improving protein crystal quality by without-oil microbatch method: crystallization and preliminary X-ray diffraction analysis of glutathione synthetase

from *Pseudoalteromonas haloplanktis*. *Int. J. Mol. Sci.*, 2011, 12, 6312–6319.

31. G. Sander, R. C. Marsh, J. Voigt and A. Parmeggiani, A comparative study of the 50S ribosomal subunit and several 50S subparticles in EF–T- and EF–G-dependent activities. *Biochemistry*, 1975, 14, 1805–1814.
32. I. Castellano, F. Cecere, A. De Vendittis, R. Cotugno, A. Chambery, A. Di Maro, A. Michniewicz, G. Parlato, M. Masullo, E. V. Avvedimento, E. De Vendittis and M. R. Ruocco, Rat mitochondrial suoperoxide dismutase: amino acid positions involved in covalent modifications, activity, and heat stability. *Biopolymers*, 2009, 91 1215–1226.
33. M. M. Bradford, A rapid and sensitive method for the quantitation of microgram quantities of protein utilizing the principle of protein–dye binding. *Anal. Biochem.*, 1976, 72, 248–254.
34. U. K. Laemmli, Cleavage of structural proteins during the assembly of the head of bacteriophage T4. *Nature*, 1970, 227, 680–685.
35. R. Dosi, A. Di Maro, A. Chambery, G. Colonna, S. Costantini, G. Geraci and A. Parente, Characterization and kinetics studies of water buffalo (Bubalus bubalis) myoglobin. *Comp. Biochem. Physiol. B, Biochem. Mol. Biol.*, 2006, 145, 230–238.
36. I. Castellano, A. Di Maro, M. R. Ruocco, A. Chambery, A. Parente, M. T. Di Martino, G. Parlato, M. Masullo and E. De Vendittis, Psychrophilic superoxide dismutase from *Pseudoalteromonas haloplanktis*: biochemical characterization and identification of a highly reactive cysteine residue. *Biochimie*, 2006, 88, 1377–1389.
37. T. E. Creighton, Disulphide bonds between cysteine residues, in *Protein structure a practical approach*, ed. T. E. Creighton, Oxford University Press, Oxford, UK, 1989, pp 155–167.
38. R. Cotugno, M. R. Ruocco, S. Marco, P. Falasca, G. Evangelista, G. Raimo, A. Chambery, A. Di Maro, M. Masullo and E. De Vendittis, Differential cold–adaptation among protein components of the thioredoxin system in the psychrophilic

eubacterium *Pseudoalteromonas haloplanktis* TAC 125. *Mol. BioSyst.*, 2009, 5, 519–528.

39. G. F. Seelig and A. Meister, Glutathione biosynthesis: γ-glutamylcysteine synthetase from rat kidney, *Methods Enzymol.*, 1985, 113, 379–390.
40. M. M. Corsaro, R. Lanzetta, E. Parrilli, M. Parrilli, M. L. Tutino and S. Ummarino, Influence of growth temperature on lipid and phosphate contents of surface polysaccharides from the Antarctic bacterium *Pseudoalteromonas haloplanktis* TAC 125. *J. Bacteriol.*, 2004, 186, 29–34.
41. H. Gushima, T. Miya, K. Murata and A. Kimura, Purification and characterization of glutathione synthetase from *Escherichia coli* B. *J. Appl. Biochem.*, 1983, 5, 210–218.
42. N.E. Chayen, P.D. Shaw Stewart, D.L. Maeder, D.M. Blow, An automated system for micro-batch protein crystallization and screening, *J. Appl. Cryst.*, 1990, 23, 297–302.
43. N.E. Chayen, Recent advances in methodology for the crystallization of biological maromolecules, *J. Cryst. Growth*, 1999, 199, 649–655.
44. P.M. Martins, J. Pessoa, Z. Sarkany, F. Rocha, A.M. Damas, Rationalizing protein crystallization screenings through water equilibration theory and protein solubility data, *Cryst. Growth Des.*, 2008, 8, 4233–4243.
45. H. Yamaguchi, H. Kato, Y. Hata, T. Nishioka, A. Kimura, J. Oda and Y. Katsube, Three-dimensional structure of the glutathione synthetase from *Escherichia coli* B at 2.0 Å resolution, *J. Mol. Biol.*, 1993, 229, 1083–1100.
46. T. Hara, H. Kato, Y. Katsube and J. Oda, A pseudo-Michaelis quaternary complex in the reverse reaction of a ligase: structure of *Escherichia coli* B glutathione synthetase complexed with ADP, glutathione, and sulfate at 2.0 Å resolution, *Biochemistry*, 1996, 35, 11967–11974.
47. K. Matsuda, K. Mizuguchi, T. Nishioka, H. Kato, N. Go and J. Oda, Crystal structure of glutathione synthetase at optimal pH: domain architecture and structural similarity with other proteins, *Protein Eng.*, 1996, 9, 1083–1092.

48. S. Srimathi, G. Jayaraman, G. Feller, B. Danielsson and P. R. Narayanan, Intrinsic halotolerance of the psychrophilic α-amylase from *Pseudoalteromonas haloplanktis*, *Extremophiles*, 2007, 11, 505–515.
49. G. Evangelista, P. Falasca, I. Ruggiero, M. Masullo and G. Raimo, Molecular and functional characterization of polynucleotide phosphorylase from the Antarctic eubacterium *Pseudoalteromonas haloplanktis*. *Protein Pept. Lett.*, 2009, 16, 999–1005.
50. T. Tanaka, T. Nishioka and J. Oda, Nicked multifunctional loop of glutathione synthetase still protects the catalytic intermediate. *Arch. Biochem. Biophys.*, 1997, 339, 151–156.
51. C. W. Nakagawa, N. Mutoh and Y. Hayashi, Glutathione synthetase from the fission yeast. Purification and its unique heteromeric subunit structure. *Biochem. Cell. Biol.*, 1993, 71, 447–453.
52. J. M. Jez and R. E. Cahoon, Kinetic mechanism of glutathione synthetase from *Arabidopsis thaliana*, *J. Biol. Chem.*, 2004, 279, 42726–42731.
53. A. Dinescu, T. R. Cundari, V. S. Bhansali, J.–L. Luo and M. E. Anderson, Function of conserved residues of human glutathione synthetase: implications for the ATP-grasp enzymes, *J. Biol. Chem.*, 2004, 279, 22412–22421.

List of publications of Dr. Albino during Doctoral training

Full publications

1. Merlino A, Russo Krauss I, **Albino A**, Pica A, Vergara A, Masullo M, De Vendittis E, Sica F
   Improving protein crystal qualità by the without-oil microbatch method: crystallization and preliminary X-Ray diffraction analysis of glutathione synthetase from *Pseudoalteromonas haloplanktis*
   International Journal of Molecular Sciences **12** (2011) 6312–6319.
2. De Vendittis A, Marco S, Di Maro A, Chambery A, **Albino A**, MasulloM, Michniewicz A, Parlato G, De Angelis A, De Vendittis E, Rullo R
   Properties of a putative cambialistic superoxide dismutase from the aerotolerant bacterium *Streptococcus thermophilus* strain LMG 18311
   Protein & Peptide Letters (2011) in press.

Abstracts of International Meetings

3. **Albino A**, Marco S, De Vendittis E, Masullo M
   The glutathione biosynthesis in the psychrophile *Pseudoalteromonas haloplanktis*
   36th FEBS Congress, Torino, June 25-30, 2011
   FEBS Journal **278**, **suppl. 1**, 389 (Abs. P26.1).
4. Marco S, **Albino A**, De Vendittis A, Rullo R, De Vendittis E
   Biochemical properties of the superoxide dismutase from the pathogenic bacterium *Helicobacter pylori*
   36th FEBS Congress, Torino, June 25-30, 2011
   FEBS Journal **278**, **suppl. 1**, 399 (Abs. P26.33).

Abstracts of National Meetings

5. Marco S, **Albino A**, Martucci NM, Rullo R, De Vendittis E
   Caratterizzazione biochimica della superossido dismutasi dal batterio patogeno *Helicobacter pylori*
   Giornate Scientifiche 2010, Polo delle Scienze e Tecnologie per la Vita, 25-26 novembre 2010, Astract n. 056.

6. **Albino A**, Lamberti A, Rullo R, De Vendittis E, Masullo M
   Il sistema preposto alla sintesi del glutatione nell'eubatterio psicrofilo *Pseudoalteromonas haloplanktis*
   Giornate Scientifiche 2010, Polo delle Scienze e Tecnologie per la Vita, 25-26 novembre 2010, Astract n. 070.
7. Merlino A, Russo Krauss I, Pica A, Vergara A, **Albino A**, Masullo M, De Vendittis E, Sica F
   The first X-Ray structure of a cold-adapted glutathione synthetase
   XXIV Congresso Nazionale della Società Chimica Italiana, Lecce 11-16 settembre 2011, Abs. FIS-PO-43, p. 575.